UDC 54-386:547.497.1

T. V. Koksharova*, A. Yu. Kovalov
Odesa I. I. Mechnikov National University,
Department of Inorganic Chemistry and Chemical Education,
2 Zmiienka Vsevoloda St, Odesa, 65082, Ukraine;
* e-mail: tanya.koksharova@gmail.com

COORDINATION COMPOUNDS OF 3d METALS CINNAMATES WITH THIOSEMICARBAZIDE: SYNTHESIS, CHARACTERIZATION AND DFT STUDY

Synthesis methods were developed, five new coordination compounds were isolated and investigated: $[CuL_2](Cinn)_2$, $[NiL_n](Cinn)_2$ (n = 2, n = 4, $[ZnL_2](Cinn)_2$, $[CoL_3](Cinn)_3$, where L — thiosemicarbazide, HCinn — cinnamic acid. The structures of the compounds were determined by FTIR and Raman spectroscopy and confirmed by quantum chemical methods. IR spectra and molecular and electronic properties of compounds were calculated by Density Functional Theory (DFT) method. Molecular orbital energies (HOMO and LUMO), energy gaps (ΔE), and global reactivity descriptors (chemical potential **μ**, chemical hardness **η**, electrophilicity index **ω**, and global softness **S**) values are determined. The reactivities and electronic structures of compounds vary depending on the metal nature.

Keywords: Thiosemicarbazide, cinnamate, Density Functional Theory

Thiosemicarbazide is a well-known complexing agent that has various valuable properties and is used in different areas [1–3]. The composition and coordination polyhedra of thiosemicarbazide complexes are strongly influenced by the anions of the salts taken for synthesis [2, 4, 5]. It is of interest to expand the range of anions for the synthesis of thiosemicarbazide complexes. We have chosen cinnamate anion. Cinnamic acid and its derivatives occur widely in nature [6, 7] and are likely to interact with metal ions [8]. They are natural compounds with a variety of biological actions [6, 9] that have a wide range of current and potential applications [10, 11]. Coordination compounds involving the cinnamate anion have not been sufficiently studied. They have been studied only with nitrogen-containing ligands. In coordination compounds with nitrogen-containing ligands, cinnamate anions can act as monodentate, bidentate, and bridging anions [12–14]. We did not find any information in the literature about coordination compounds of cinnamates with sulfur-containing ligands. This study aims to synthesize coordination compounds of 3d-metal cinnamates with thiosemicarbazide and study their structure using spectral and quantum-chemical methods.

EXPERIMENTAL SECTION

All reagents and solvents were of reagent grade quality and were obtained from commercial suppliers. $CuCl_2{\cdot}2H_2O$, $NiCl_2{\cdot}6H_2O$, $CoCl_2{\cdot}6H_2O$, $ZnSO_4{\cdot}7H_2O$, cinnamic acid C_6H_5–CH=CH–COOH, thiosemicarbazide $NH_2NHC(S)NH_2$.

Nitrogen content was carried out on a LECO Tru Spec CHN automatic elemental analyzer. The contents of the metal ions were determined by inductively coupled

https://doi.org/10.18524/2304-0947.2025.2(90).352366

plasma atomic emission spectrometry (ICP-AES) on a Perkin-Elmer Optima 8000 analyzer, the sulfur content by the Schoeniger method.

IR spectra were recorded on a Perkin-Elmer SPECTRUM BX II FT-IR SYSTEM spectrometer at the range of 4000–400 cm^{-1} at room temperature in KBr pellets.

Raman spectra were obtained on a DXR Raman Microscope, Thermo Scientific using a laser with a wavelength of 532 nm, laser power of 10 mW, with a full-band grating, in the Stokes region range of 3360–200 cm^{-1}. The sample was placed on a microscope glass slide, focused with a laser.

Synthesis of $[CuL_2](Cinn)_2$. A portion of $Cu(Cinn)_2$ (1.8 g, 5 mmol) was added to a solution of L (0.91 g, 10 mmol). The solution turned dark blue, and a light brown precipitate formed. After cooling, the light-brown precipitate was filtered off, washed with a small amount of water and ethanol and dried in air to constant weight.

Synthesis of $[NiL_2](Cinn)_2$, $[NiL_4](Cinn)_2$, $[ZnL_2](Cinn)_2$, $[CoL_3](Cinn)_3$. A solution of NaOH (0.4 g, 10 mmol) in 5 mL of water was added drop by drop to 5 mmol of corresponding metal salt in 5 mL of water. The precipitate of $M(OH)_2$ (M = Ni, Zn, Co) formed was filtered off, washed with a small amount of water and 20 mL of ethanol and added to a warm solution of cinnamic acid (1.48 g, 10 mmol) in 50 mL of water until complete dissolution. Finely ground L in a ratio of 1:2 ($[NiL_2](Cinn)_2$, $[ZnL_2](Cinn)_2$), 1:4 ($[NiL_4](Cinn)_2$), 1:3 ($[CoL_3](Cinn)_3$) was added in portions to the mixture and left for 1 hour ($[NiL_2](Cinn)_2$, $[NiL_4](Cinn)_2$, $[ZnL_2](Cinn)_2$) and for a day ($[CoL_3](Cinn)_3$). Precipitates formed was filtered off, washed with a small amount of water and ethanol and dried in air to constant weight.

RESULTS AND DISCUSSION

According to the data of the elemental analysis (Table 1) the products isolated have molar ratio Metal : L : Cinnamate 1:2:2 for copper and zinc (compounds **I** and **IV**), 1:3:3 for cobalt (compound **V**), whereas for nickel, depending on the ratio of reagents, two compositions are realized: 1:2:2 (compound **II**) and 1:4:2 (compound **III**).

Table 1

The elemental analysis data and colors of complexes

N	Compound	M, %		N, %		S, %		Color
		Found	Calculated	Found	Calculated	Found	Calculated	
I	$[CuL_2](Cinn)_2$	11.88	11.85	15.51	15.56	11.80	11.85	Light- brown
II	$[NiL_2](Cinn)_2$	11.04	11.03	15.56	15.70	11.95	11.96	Pink
III	$[NiL_4](Cinn)_2$	8.26	8.23	23.51	23.43	17.90	17.85	Green
IV	$[ZnL_2](Cinn)_2$	12.11	12.01	15.51	15.53	11.88	11.83	Light-pink
V	$[CoL_3](Cinn)_3$	7.64	7.63	16.21	16.30	12.46	12.42	Black

Analysis of the IR and Raman spectra of the obtained compounds compared to initial substances (L, metal cinnamates) made it possible to obtain information the nature of bonds in **I–V**.

Experimental and calculated results of the most characteristic corresponding assignments of compounds are listed in Table 2, 3. Thiosemicarbazide (L) is ambidentate ligand that can form five-membered metal cycles (with N,S or N,N coordination cores) or can be bonded in monodentate type through S atom. The ligand contains thioamide bands at the following frequencies (cm^{-1}): thioamide I — 1530, thioamide II — 1315, thioamide III — 1000, thioamide IV — 800. The analysis of IR spectra of L and of the products of its reactions with 3d-metals cinnamates shows that the **III** spectrum differs from the spectra of all other compounds. In the **I**, **II**, **IV**, **V** spectra, the band thioamide II shifts to the region of higher frequencies by 65–70 cm^{-1} as compared to L, while the frequency thioamide IV lowers down by 20–31 cm^{-1}. The intensity of the thioamide II band increases due to the fact that the vibrations of the cinnamate-anions also contribute to it. The thioamide I band is shifted to the high-frequency region by 47–48 cm^{-1} with significant decreasing intensity. The thioamide III band sharply lowers the intensity, so that for **I** and **II**, it turns into a shoulder, and for **IV** completely disappears. Such a change in thioamide bands is known to correspond to bidentate coordination of the ligands with participation of S and N atoms [15].

For the compound **III**, the spectrum is significantly different. Tioamide IV band lowers the frequency. Tioamide I shift is much smaller than in the spectra of all other compounds. The thioamide II band almost does not change, and thioamide III sharply lowers the intensity. Therefore, one can conclude that in **III**, L has monodentate coordination through the S atom to give NiS_4 coordination core.

In the Raman spectra, the thioamide IV band lowers its frequency by 30–38 cm^{-1}, thioamide II rises by 71–87 cm^{-1}. The shifts of these bands in the Raman spectrum are significantly smaller for a zinc complex. The thioamide III band in the Raman spectrum of the ligand is observed at a lower frequency — 992 cm^{-1}, and for complexes in Raman spectra it is observed at the same frequencies as in the IR spectra, and the zinc compound differs here too. In all cases, thioamide III degenerates into the shoulder. Consequently, the shifts of thioamide bands are quite close to the IR and the Raman spectra.

The area of low frequencies in the Raman Spectra is very useful for interpretation of the metal-ligand bonds. For **III** in the Raman spectrum there are no bands ν (M–N) and δ(M–N–N) + ν (M–S), that confirms the absence of nickel bond through nitrogen. In the area of thioamide bands, the spectrum of **III** is characterized by a smaller shift of the thioamide II band.

The value of the difference between frequencies $\nu_{as}(COO^-)$ and $\nu_s(COO^-)$ can be successfully used to determine the nature of binding carboxylate. The value of $\Delta\Delta\nu(COO^-)$ represents the difference in $\nu(COO^-)$ values between a mixed-ligand complex and an initial metal carboxylate. Greater $\Delta\Delta\nu(COO^-)$ values are observed for monodentate carboxylate anions and much lower, for bidentate and outer-sphere anions. In all cases, the values of $\Delta\Delta\nu(CO_2)$ are insignificant, and for cobalt (III) this value is even negative, which is consistent with the outer character of anion.

Computation details. Theoretical calculations were performed using the **ORCA 6.00** software [16] package within the framework of density functional theory (DFT), employing the hybrid B3LYP [17, 18] functional in combination with

ISSN 2304-0947

Table 2

Comparison of experimental and calculated FTIR results (in cm^{-1}) for copper(II) and nickel(II) complexes

	$[Cu(TSC)_2](Cinn)_2$			$[Ni(TSC)_2](Cinn)_2$			$[Ni(TSC)_4](Cinn)_2$		
	Calc. IR	**Exp. IR**	**Raman**	**Calc. IR**	**Exp. IR**	**Raman**	**Calc. IR**	**Exp. IR**	**Raman**
ν(NH)	3370, 3074	3303, 3260, 3236	3197, 3156, 3089, 3067, 3036	3282, 3101, 3074	3347, 3189, 3049 , 3034		3463, 3282, 3135, 3046, 2949	3417, 3085, 3059, 3025	3196, 3089, 3066, 3037
Thioamide I	1598	1578	1602	1597	1577	1576	1563	1550	1604
Thioamide II	1360	1385	1371	1363	1384*	1387	1302	1316	1328
Thioamide III	1000 shoulder	1000 shoulder	1000 shoulder	1000 shoulder	1000 shoulder	1000 shoul-der	1000 shoulder	1000 shoulder	1001 shoulder
Thioamide IV	738	769	770	780	780	778	761	767	770
ν(CH)	3074, 2700	3197, 3156, 3089, 3067, 3036	3067, 3036	3101, 3074	3049, 3034	3059, 3004	3135, 3046, 2949	3089, 3066, 3037	3089, 3066, 3037
$\nu(C{=}C_{alkene})$	1598	1602	1626	1638	1633	1633	1640	1620	1620
$\nu(C{=}C_{arene})$	1360	1371	1496	1484, 1439	1498, 1449	1500	1511, 1437	1494, 1443	1494, 1443
$\nu_{as}(CO_2)$	1636	1630		1638	1633	1633	1640	1620	1620
$\nu_{s}(CO_2)$	1360	1385	1371	1363	1384*	1387	–	–	–
$\delta(CO_2)$	1238	1286	1291	1248	1291	1291	1302	1288	1292

*Overlapping bands of thiosemicarbazide and cinnamate anions

Table 3

Comparison of experimental and calculated FTIR results (in cm^{-1}) for zinc(II) and cobalt(III) complexes

	$[Zn(TSC)_2](Cinn)_2$			$[Co(TSC)_3](Cinn)_3$		
	Calc. IR	**Exp. IR**	**Raman**	**Calc. IR**	**Exp. IR**	**Raman**
ν(NH)	3448, 3184, 3033, 3018	3451, 3278, 3195, 3060, 3027	3258, 3180	3406, 3283, 3144	3438, 3139	3195, 3088, 3067, 3036
Thioamide I	1554	1578	1599	1577	1578	1602
Thioamide II	1372	1380	1316	1362	1385	1373
Thioamide III	–	–	989	1001	1001	1001
Thioamide IV	791	774	806	738	769	770
ν(CH)	3033, 3018, 2652,2653	3060, 2957	3060, 2957	2970, 2609, 2611, 2613	3036, 2985	3036, 2985
$\nu(C{=}C_{alkene})$	1661	1640	1638	1638	1640	1627
$\nu(C{=}C_{arene})$	1505, 1482	1496, 1450	–	1531	1494, 1442	1494, 1442
$\nu_{as}(CO_2)$	1661	1640	1638	1638	1627	1627
$\nu_s(CO_2)$	1396	1395	–	1438	1420	
$\delta(CO_2)$	1271	1276	1265	1307	1287	1290

the def2-TZVP basis set and the def2/J auxiliary basis set for all elements [19]. Stationary points verification of the molecular structures as a global minimum are performed by frequency calculation with no imaginary frequencies. Conductor like Polarizable Continuum Model (CPCM) [20], an implicit solvent model, is used with the intention of understanding solvent effect. Solvents are H_2O, 50% water solution of CH_3OH with the dielectric constant values 78.5 and 51.22 respectively. Lichtenecker's Logarithmic Mixture Formula Eq. (1) [21] was used for calculation of dielectric constants CH_3OH water solution:

$$\epsilon_{mix} = exp\left(\sum_i\right) V_i ln(\epsilon_i) \quad (1)$$

Frequency calculation was performed in gas phase.

Chemcraft [22] and Avogadro [23] software were used for visualization of the calculations.

Geometric optimization and calculation of vibration frequencies were performed taking into account the effect of the solvent. Fig. 1–5 show the geometry and Table 4 shows the bond lengths and angles in cinnamate-thiosemicarbazide compounds.

I exhibits a square-planar coordination environment, **II** has distorted square structure, **III** and **IV** adopt a distorted tetrahedral geometry, while the Co(III) complex

V assumes an octahedral geometry. The transition from a square to a tetrahedral structure with a change in the nickel-ligand ratio from 1:2 to 1:4 is explained by the larger radius of the sulfur atom compared to the nitrogen atom.

The convergence of experimental and theoretical spectroscopy results (Table 2, 3) confirms the reliability of the assumptions about the structures of the synthesized compounds.

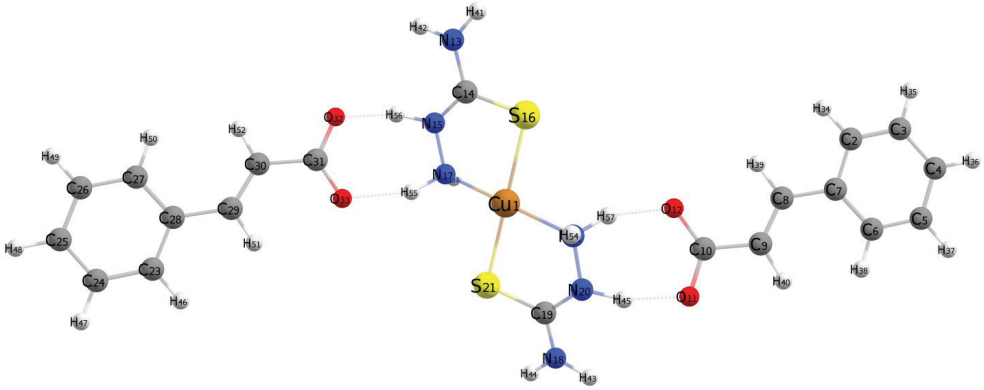

Fig. 1. Optimized structure of $[CuL_2](Cinn)_2$ (**I**)

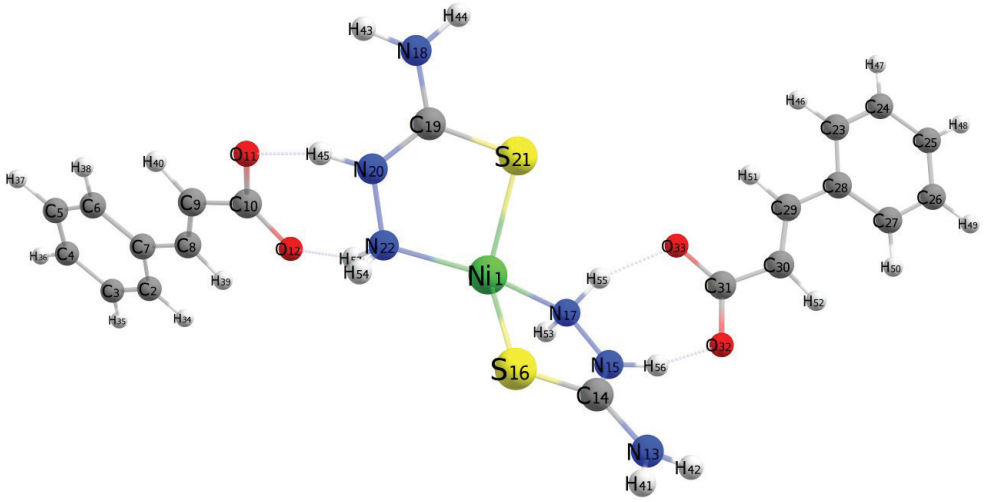

Fig. 2. Optimized structure of $[NiL_2](Cinn)_2$ (**II**)

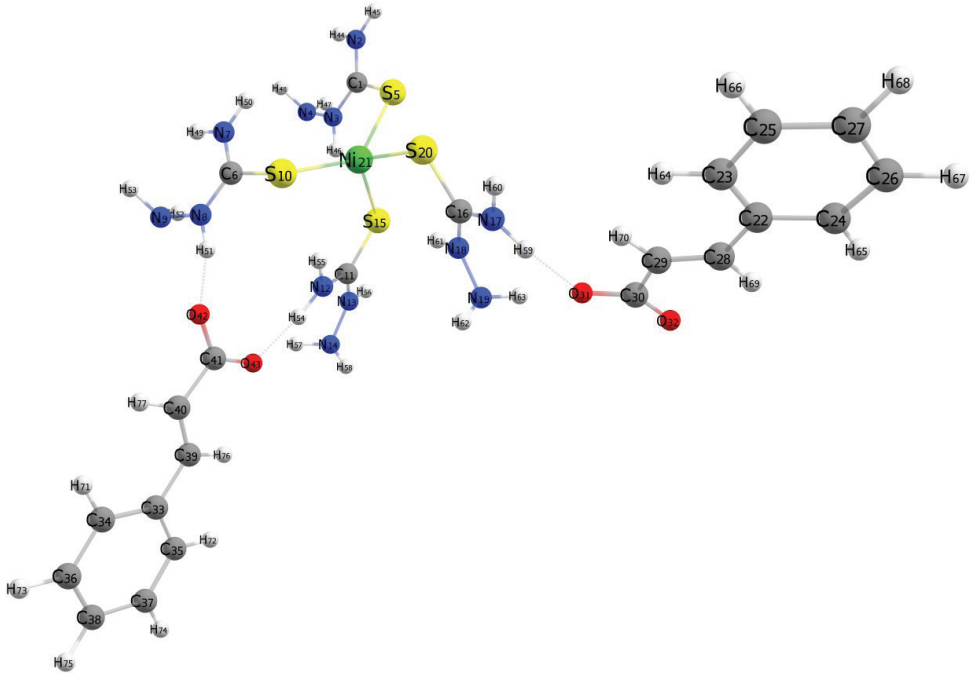

Fig. 3. Optimized structure of $[NiL_4](Cinn)_2$ (**III**)

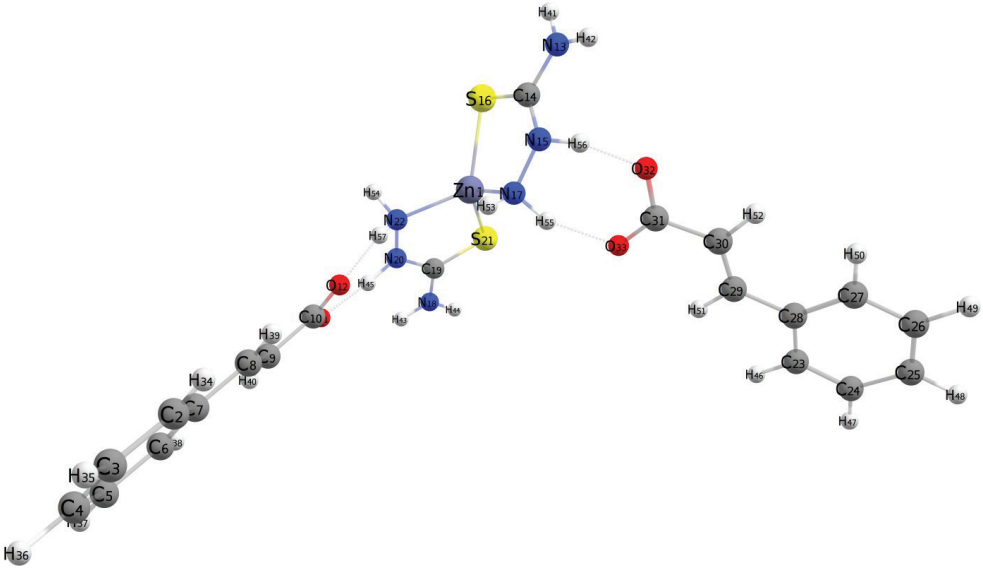

Fig. 4. Optimized structure of $[ZnL_2](Cinn)_2$ (**IV**)

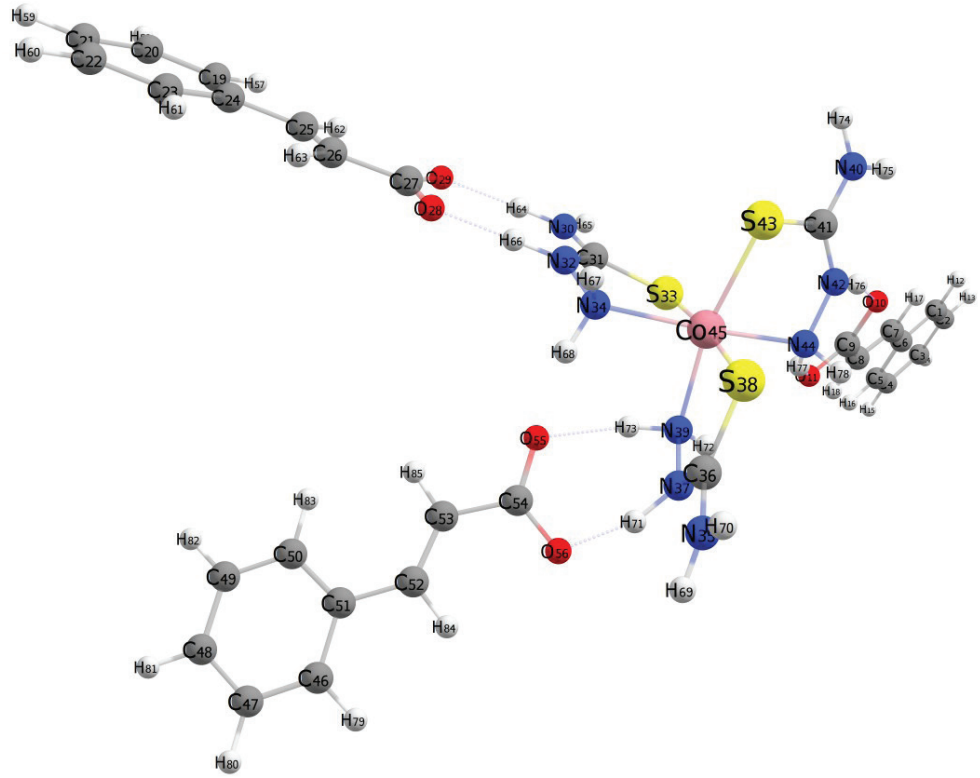

Fig 5. Optimized structure of $[CoL_3](Cinn)_3$ (**V**)

Overall, the discrepancies between calculated and experimental values did not exceed 57 cm^{-1}, which is acceptable for DFT-based methods. The largest deviations were observed for $[CuL_2](Cinn)_2$, particularly for thioamide II (57 cm^{-1}) and thioamide IV (32 cm^{-1}). Significant shifts were also found in $[NiL_2](Cinn)_2$, where thioamide II and IV differed by 21 cm^{-1} and 26 cm^{-1}, respectively. In contrast, $[CoL_3](Cinn)_3$ exhibited the most accurate results, with all deviations under 12 cm^{-1}. These findings suggest that the computational method better reproduces spectral features for complexes with higher coordination numbers.

Table 4

Selected bond lengths d and angles ω in structures I–V

I			
Bond	d, Å	Bond	d, Å
Cu1–S21	2.336	H56–O32	1.631
Cu1–S16	2.336	H45–O11	1.631
Cu1–N22	2.030	H57–O12	1.804

Table 4 (continuing)

Cu1–N17	2.030	C31–O32	1.272
N17–N15	1.414	C31–O33	1.262
N15–C14	1.327	C31–C30	1.496
C14–N13	1.332	C30–C29	1.339
C14–S16	1.727	C29–C28	1.465
N22–N20	1.414	Angles	ω, deg
N20–C19	1.327	N17–Cu1–S16	85.18
C19–N18	1.332	N17–Cu1–S21	94.81
C19–S21	1.727	S21–Cu1–N22	85.18
H55–O33	1.805	N22–Cu1–S16	94.82
II			
Bond	d, Å	Bond	d, Å
Ni1–S21	2.306	H56–O32	1.631
Ni1–S16	2.311	H45–O11	1.644
Ni1–N22	2.047	H57–O12	1.810
Ni1–N17	2.045	C31–O32	1.272
N17–N15	1.417	C31–O33	1.260
N15–C14	1.326	C31–C30	1.497
C14–N13	1.331	C30–C29	1.339
C14–S16	1.731	C29–C28	1.465
N22–N20	1.417	Angles	ω, deg
N20–C19	1.327	N17–Ni1–S16	86.14
C19–N18	1.331	N17–Ni1–S21	105.00
C19–S21	1.730	S21–Ni1–N22	86.41
H55–O33	1.819	N22–Ni1–S16	103.97
III			
Bond	d, Å	Bond	d, Å
Ni21–S5	2.364	C1–N3	1.334
Ni21–S20	2.384	N3–N4	1.400
Ni21–S15	2.329	H59–O31	1.758

Table 4 (continuing)

Ni21–S10	2.350	H51–O42	1.754
S20–C16	1.736	H54–O43	1.705
C16–N17	1.327	C30–O31	1.276
C16–N18	1.333	C30–O32	1.249
N18–N19	1.406	C30–C29	1.505
S15–C11	1.754	C29–C28	1.338
C11–N12	1.313	C28–C22	1.466
C11–N13	1.336	C41–O42	1.264
N13–N14	1.403	Angles	ω, deg
S10–C6	1.753	S20–Ni21–S5	92.08
C6–N7	1.326	S20–Ni21–S15	115.28
C6–N8	1.324	S20–Ni21–S10	94.82
N8–N9	1.406	S5–Ni21–S10	136.87
S5–C1	1.735	S10–Ni21–S15	116.33
C1–N2	1.326	S15–Ni21–S5	98.55
IV			
Bond	d, Å	Bond	d, Å
Zn1–S21	2.359	H56–O32	1.644
Zn1–S16	2.362	H45–O11	1.652
Zn1–N22	2.095	H57–O12	1.814
Zn1– N17	2.091	C31–O33	1.260
N17–N15	1.414	C31–O32	1.272
N15–C14	1.332	C31–C30	1.498
C14–N13	1.333	C30–C29	1.339
C14–S16	1.728	C29–C28	1.465
N22–N20	1.414	Angles	ω, deg
N20–C19	1.331	N17–Zn1–S16	86.39
C19–N18	1.333	N17–Zn1–S21	123.75
C19–S21	1.729	S21–Zn1–N22	86.27
H55–O33	1.823	N22–Zn1–S16	120.14

Table 4 (continuing)

V			
Bond	d, Å	Bond	d, Å
Co45–S33	2.288	H71–O56	1.610
Co45–N34	2.213	H76–O10	1.602
Co45–S38	2.307	H77–O11	1.849
Co45–N39	2.072	O29–C27	1.261
Co45–S43	2.328	O28–C27	1.269
Co45–N44	2.218	C27–C26	1.497
S33–C31	1.743	C26–C25	1.339
C31–N30	1.322	C25–C24	1.465
C31–N32	1.326	Angles	ω, deg
N32–N34	1.411	S33 –Co45–N34	82.14
S38–C36	1.734	N34–Co45–S38	92.75
C36–N35	1.326	S33–Co45–S43	96.93
C36–N37	1.328	S43–Co45–S38	87.12
N37–N39	1.420	S33–Co45–N44	88.72
S43–C41	1.738	N44–Co45–S38	96.46
C41–N40	1.331	S33–Co45–N39	93.56
C41–N42	1.319	N39–Co45–S38	83.1
N42–N44	1.413	N44–Co45–N39	91.33
H64–O29	1.728	N39–Co45–N34	90.75
H66–O28	1.632	N31–Co45–S43	98.4
H73–O55	1.842	S43–Co45–N44	81.14

Orbital and global reactivity analysis. The global reactivity indices of molecules are calculated using Koopman's Theorem. According to this theorem, the ionization potential and electron affinity are related to the negative values of the energies of the Highest Occupied Molecular Orbital (E_{HOMO}) and the Lowest Unoccupied Molecular Orbital (E_{LUMO}), respectively. From these, the chemical potential (μ) Eq.(2), hardness (η) Eq.(3) , electrophilicity index (ω) Eq. (4), and softness (S) Eq.(5) are computed using Eq. (2)–(5) [24].

$$\mu = \frac{(E_{HOMO} + E_{LUMO})}{2} \quad (2)$$

$$\eta = \frac{(E_{LUMO} - E_{HOMO})}{2} \quad (3)$$

$$S = \frac{1}{2\eta} \quad (4)$$

$$\omega = \frac{\mu^2}{2\eta} \quad (5)$$

The data presented in the Table 5 and Fig. 6 demonstrate and diagram significant variations in the frontier molecular orbital energies (HOMO and LUMO), energy gaps (ΔE), and global reactivity descriptors (chemical potential **μ**, chemical hardness **η**, electrophilicity index **ω**, and global softness **S**) among the ligand L and its metal complexes.

The free ligand L exhibits a large energy gap (ΔE = 9.44 · 10^{-19} J), the HOMO is primarily localized on the sulfur and hydrazinic nitrogen atoms, while the LUMO resides at a much higher energy level, supporting its role as an electron donor with limited acceptor ability.

Table 5

The global reactivity indices of molecules

Compound	E_{HOMO} ·10^{19}, J	E_{LUMO} ·10^{19}, J	ΔE ·10^{19}, J	μ ·10^{19}, J	η ·10^{19}, J	ω · 10^{19}, J	S · 10^{19}, J^{-1}	E_{HOMO} ·10^{19}, J
$[CuL_2](Cinn)_2$	−10.89	−1.54	9.36	−6.21	4.68	4.13	0.11	−10.89
$[NiL_2](Cinn)_2$	−10.38	−6.53	3.85	−8.46	1.93	18.57	0.26	−10.38
$[NiL_4](Cinn)_2$	−9.77	−6.75	3.02	−8.26	1.51	22.6	0.33	−9.77
$[ZnL_2](Cinn)_2$	−11.58	−1.65	9.93	−6.61	4.96	4.4	0.1	−11.58
$[CoL_3](Cinn)_3$	−11.86	−11.63	0.23	−11.75	0.12	597.22	4.33	−11.86

The Cu(II) and Zn(II) complexes retain similarly large energy gaps (9.36 · 10^{-19} J and 9.93 · 10^{-19} J, respectively), with frontier orbitals mainly localized on the ligand framework. These values suggest that these complexes are electronically stable and chemically inert under standard conditions. Their relatively low electrophilicity indices (ω ≈ 4.1–4.4 · 10^{-19} J) and small global softness values support this assessment.

In contrast, the Ni(II) complexes — $[NiL_2]^{2+}$ and $[NiL_4]^{2+}$ — exhibit intermediate energy gaps of 3.82 · 10^{-19} J and 3.02 · 10^{-19} J, respectively. This indicates moderate reactivity, which is corroborated by higher electrophilicity indices (ω = 18.57 · 10^{-19} J and 22.6 · 10^{-19} J) and greater softness (**S** = 0.26 · 10^{-19} J^{-1} and 0.23 · 10^{-19} J^{-1}). These complexes also show delocalization of the frontier orbitals across both metal centers and ligand atoms, facilitating electron density redistribution and thus enhancing reactivity.

The Co(III) complex is distinguished by an extremely narrow energy gap (ΔE = 0.23 · 10^{-19} J), the lowest among all species examined. This narrow gap correlates with a remarkably high electrophilicity index (ω = 597.22 · 10^{-19} J) and high softness

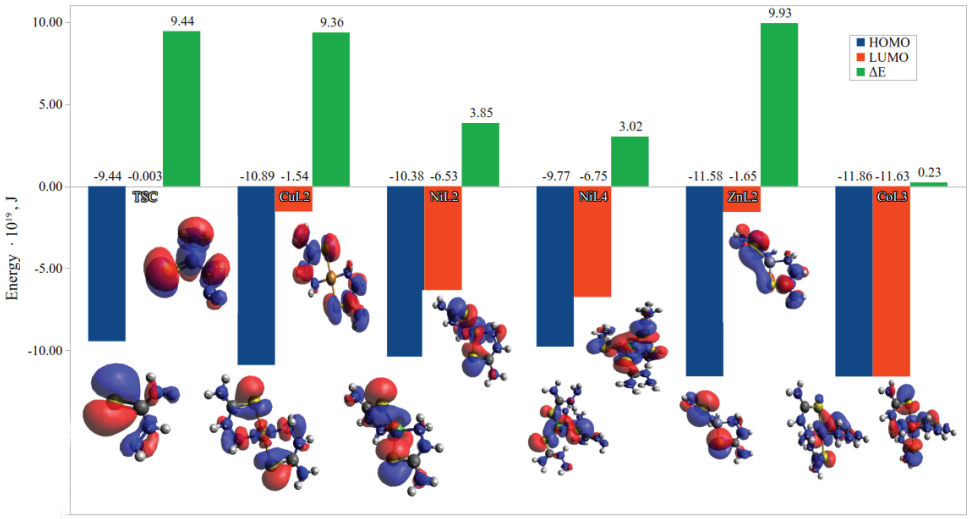

Fig. 6. Frontier molecular orbitals and energy gaps of molecules

($\mathbf{S} = 4.33 \cdot 10^{-19}\ J^{-1}$), clearly indicating pronounced chemical reactivity. The frontier orbitals in this complex are strongly delocalized over both metal and ligand, further supporting the interpretation of enhanced electronic communication and reactivity.

In summary, the trend in reactivity follows the inverse order of energy gap magnitude: **CoL_3 >> NiL_4 ≈ NiL_2 > CuL_2 ≈ ZnL_2**, with CoL_3 standing out as a highly reactive species, and Cu(II)/Zn(II) complexes exhibiting notable stability.

Thus, five new coordination compounds of 3d-metal cinnamates with thiosemicarbazide were synthesized. Characterization of all compounds by spectroscopic methods (FTIR, Raman) was examined and their electronic properties were calculated by quantum chemical methods. The results of experimental and quantum chemical calculations are in good agreement, that confirms the assumptions about the structures of the synthesized compounds.

It has been found the significant variations in the frontier molecular orbital energies (HOMO and LUMO), energy gaps (ΔE), and global reactivity descriptors (chemical potential **μ**, chemical hardness **η**, electrophilicity index **ω**, and global softness **S**) between the ligand and its metal complexes.

The results obtained show that the nature of the metal is the deciding factor in the formation of coordination compounds as well in their reactivity.

REFERENCES

1. Leovac V. M., Novaković S. B. Versatile coordination chemistry of thiosemicarbazide and its non-Schiff base derivatives. *J. Mol. Struct*. 2024, *1314*, 138721. https://doi.org/10.1016/j.molstruc.2024.138721
2. Campbell M. J. M. Transition metal complexes of thiosemicarbazides and thiosemicarbazones. *Coord. Chem. Revs*. 1975, *15*(2–3), 279–319.
3. Acharya P. T., Bhavsar Z. A., Jethava D. J., Patel D. B., Patel H. D. A review on development of bio-active thiosemicarbazide derivatives: recent advances. *J. Mol. Struct*. 2021, *1226 A*, 129268. https://doi.org/10.1016/j.molstruc.2020.129268

4. Sadikov G. G., Antsyshkina A. S., Koksharova T. V., Sergienko V. S., Kurando S. V., Gritsenko I. S. Synthesis and crystal structure of thiosemicarbazide complexes of nickel(II) and copper(II). *Crystallogr. Rep*. 2012, *57*(4), 528–540. https://doi.org/10.1134/S1063774512030170
5. Koksharova T. V. O vliyanii aniona soli na sostav i svoystva tiosemikarbazidnykh kompleksov 3d-metallov [The effect of a salt anion on a composition and properties of 3d-metals thiosemicarbazide complexes]. *Vìsn. Odes. nac. unìv., Hìm.* [Odesa National University Herald. Chemistry]. 2003, 8(4), 192–199. [in Russian].
6. Yang S., Zhang Y., Wang Y., Qin R., Chen Y., Hu H., Liu Z., Hu Y., Hua Q., Wu Y., Liu Z. A study of antibacterial activity and mechanism of potassium cinnamate intended as a natural preservative. *LWT*. 2025, *215*, 117237. https://doi.org/10.1016/j.lwt.2024.117237
7. Zeleňák V., Císařová I., Llewellyn P. Diversity of carboxylate coordination in two novel zinc(II) cinnamate complexes. *Inorg. Chem. Comm*. 2007, *10*(1), 27–32. https://doi.org/10.1016/j.inoche.2006.08.021
8. Drew M. G. B., Mullins A. P., Rice D. A. Synthesis, characterization and structural properties of some copper(II) trans-cinnamates and related compounds. *Polyhedron*. 2007, *13*(10), 1631–1637. https://doi.org/10.1016/s0277-5387(00)83459-2
9. Kalinowska M., Świsłocka R., Lewandowski W. The spectroscopic (FT-IR, FT-Raman and 1H, 13C NMR) and theoretical studies of cinnamic acid and alkali metal cinnamates. *J. Mol. Struct*. 2007, *834–836*, 572–580. https://doi.org/10.1016/j.molstruc.2006.11.043
10. Crowther D., Chowdhury M., Kariuki B. M. Layering in cinnamate structures: The role of cations and anion substituents. *J. Mol. Struct*. 2008, *872*(1), 64–71. https://doi.org/10.1016/j.molstruc.2007.02.022
11. Mohsin S. M. N., Hussein M. Z., Sarijo S. H., Fakurazi S., Arulselvan P., Hin T.-Y.Y. Synthesis of (cinnamate-zinc layered hydroxide) intercalation compound for sunscreen application. *Chem. Central J*. 2013, *7*(26), 26. https://doi.org/10.1186/1752-153X-7-26
12. Kondratenko Y., Zolotarev A. A., Ignatyev I., Ugolkov V., Kochina T. Synthesis, crystal structure and properties of copper(II) complexes with triethanolamine and carboxylic acids (succinic, salicylic, cinnamic). *Transit. Metal Chem*. 2020, *45*(1), 71–81. https://doi.org/10.1007/s11243-019-00359-7
13. Batoola S. S., Gilani S. R., Zainab S. S., Tahir M. N., Harrison W. T. A., Haider M. S., Syed Q., Mazhar S., Shoai M. Synthesis, crystal structure, thermal studies and antimicrobial activity of a mononuclear Cu(II)-cinnamate complex with N,N,N/,N/ tetramethylethylenediamine as co-ligand. *Polyhedron*. 2020, *178*, 114346. https://doi.org/10.1016/j.poly.2020.114346
14. Sharma R. P., Saini A., Venugopalan P., Jezierska J., Ferretti V. Rare monomeric-dimeric copper(II) cinnamate complexes in one single crystal: Syntheses, characterization, structure determination and DFT studies of two copper(II) complexes. *Inorg. Chem. Comm*. 2012, *20*, 209–213. https://doi.org/10.1016/j.inoche.2012.03.010
15. Singh B., Singh R., Chaudhary R. V., Thakur K. P. Thioamide bands and nature of bonding in transition metal complexes of ligands having a thioamide group. *Indian J. Chem*. 1973, *11*(2), 174–177.
16. Neese F., Wennmohs F., Becker U., Riplinger C. The ORCA quantum chemistry program package. *J. Chem. Phys.* 2020, *152*(22), 224108. https://doi.org/10.1063/5.0004608
17. Becke A. D. Density-functional thermochemistry. III. The role of exact exchange. *J. Chem. Phys.* 1993, *98*(7), 5648–5652. https://doi.org/10.1063/1.464913
18. Lee C., Yang W., Parr R. G. *Development of the Colle-Salvetti correlation-energy formula into a functional of the electron density. Phys. Rev. B*. 1988, *37***(**2), 785–789. https://doi.org/10.1103/PhysRevB.37.785
19. Weigend F., Ahlrichs R. *Balanced basis sets of split valence, triple zeta valence and quadruple zeta valence quality for H to Rn: design and assessment of accuracy. Phys. Chem. Chem. Phys***.** 2005, *7***(18),** 3297–3305. https://doi.org/10.1039/B508541A
20. Barone V., Cossi M. *Quantum calculation of molecular energies and energy gradients in solution by a conductor solvent model. J. Phys. Chem. A***.** 1998, *102***(**11), 1995–2001. https://doi.org/10.1021/jp9716997
21. Lichtenecker K. *Die Dielektrizitätskonstante natürlicher und künstlicher Mischkörper. Physikalische Zeitschrift*. 1926, *27***,** 115–158.
22. Chemcraft — graphical software for visualization of quantum chemistry computations. Version 1.8, build 682. https://www.chemcraftprog.com
23. Hanwell M. D., Curtis D. E., Lonie D. C., Vandermeersch T., Zurek E., Hutchison G. R. "Avogadro: An advanced semantic chemical editor, visualization, and analysis platform". *J. Cheminformatics*. 2012, *4*(1), 17. https://doi.org/10.1186/1758-2946-4-17
24. Domingo L., Ríos-Gutiérrez M., Pérez P. Applications of the conceptual density functional theory indices to organic chemistry reactivity. *Molecules*. 2016, *21*(6), 748–770. https://doi.org/10.3390/molecules21060748

Стаття надійшла до редакції 22.08.2025
Стаття прийнята до друку після рецензування 07.10.2025
Стаття опублікована 29.12.2025

Т. В. Кокшарова, А. Ю. Ковальов
Одеський національний університет імені І. І. Мечникова,
кафедра неорганічної хімії та хімічної освіти,
вул. Змієнка Всеволода, 2, м. Одеса, 65082, Україна;
e-mail: tanya.koksharova@gmail.com

КООРДИНАЦІЙНІ СПОЛУКИ ЦИННАМАТІВ 3d МЕТАЛІВ З ТІОСЕМІКАРБАЗИДОМ: СИНТЕЗ, ХАРАКТЕРИСТИКА ТА ДОСЛІДЖЕННЯ МЕТОДОМ DFT

Розроблено методи синтезу, виділено та досліджено п'ять нових координаційних сполук: $[CuL_2](Cinn)_2$, $[NiL_n](Cinn)_2$ (n = 2, n = 4, $[ZnL_2](Cinn)_2$, $[CoL_3](Cinn)_3$, де L — тіосемікарбазид, HCinn — корична кислота. Структури сполук визначено за допомогою Фур'є ІЧ-спектроскопії та спектроскопії комбінаційного розсіяння. Зміна тіоамідних смуг у сполуках $[CuL_2](Cinn)_2$, $[NiL_2](Cinn)_2$, $[ZnL_2](Cinn)_2$, $[CoL_3](Cinn)_3$ відповідає бідентатній координації лігандів за участю атомів S та N. У сполуці $[NiL_4](Cinn)_2$ L має монодентатну координацію через атом S, утворюючи координаційний вузол NiS_4. Відсутність у спектрі комбінаційного розсіювання смуг ν(M–N) та δ(M–N–N) + ν(M–S) в області низьких частот також підтверджує монодентатну координацію тіосемікарбазиду через атом сірки. Характер зміни смуг $\nu_{as}(COO^-)$ та (COO^-) у координаційних сполуках з тіосемікарбазидом порівняно з вихідними циннаматами відповідає зовнішньосферному характеру аніону. Молекулярні та електронні властивості сполук розраховано методом теорії функціоналу густини (DFT). Визначено енергії молекулярних орбіталей (HOMO та LUMO), енергетичні заборонені зони (ΔE) та значення глобальних дескрипторів реакційної здатності (хімічний потенціал μ, хімічна твердість η, індекс електрофільності ω та глобальна м'якість S). Реакційні здатності та електронні структури сполуки різняться залежно від природи металу. $[CuL_2](Cinn)_2$ має квадратно-плоский координаційний вузол, $[NiL_2](Cinn)_2$ має викривлену квадратну структуру, $[NiL_2](Cinn)_2$ та $[ZnL_2](Cinn)_2$ — викривлену тетраедричну геометрію, тоді як комплекс $[CoL_3](Cinn)_3$ октаедричний. Збіжність результатів експериментальних спектрів та теоретично розрахованих частот в ІЧ спектрах підтверджує достовірність припущень щодо структур синтезованих сполук.
Тенденція реакційної здатності відповідає зворотному порядку величини енергетичного розриву: $CoL_3 >> NiL_4 \approx NiL_2 > CuL_2 \approx ZnL_2$, де CoL_3 виділяється як високореактивна речовина, а комплекси Cu(II)/Zn(II) демонструють значну стабільність.

Ключові слова: тіосемікарбазид, циннамат, теорія функціоналу густини.

СПИСОК ЛІТЕРАТУРИ

1. Leovac V. M., Novaković S. B. Versatile coordination chemistry of thiosemicarbazide and its non-Schiff base derivatives. *J. Mol. Struct*. 2024, *1314*, 138721. https://doi.org/10.1016/j.molstruc.2024.138721
2. Campbell M. J. M. Transition metal complexes of thiosemicarbazides and thiosemicarbazones. *Coord. Chem. Revs*. 1975, *15*(2–3), 279–319.
3. Acharya P. T., Bhavsar Z. A., Jethava D. J., Patel D. B., Patel H. D. A review on development of bio-active thiosemicarbazide derivatives: recent advances. *J. Mol. Struct*. 2021, *1226 A*, 129268. https://doi.org/10.1016/j.molstruc.2020.129268
4. Sadikov G. G., Antsyshkina A. S., Koksharova T. V., Sergienko V. S., Kurando S. V., Gritsenko I. S. Synthesis and crystal structure of thiosemicarbazide complexes of nickel(II) and copper(II). *Crystallogr. Rep*. 2012, *57*(4), 528–540. https://doi.org/10.1134/S1063774512030170
5. Кокшарова Т. В. О влиянии аниона соли на состав и свойства тиосемикарбазидных комплексов 3d-металлов. *Вісник Одеського національного університету. Хімія*. 2003, *8*(4), 192–199.
6. Yang S., Zhang Y., Wang Y., Qin R., Chen Y., Hu H., Liu Z., Hu Y., Hua Q., Wu Y., Liu Z. A study of antibacterial activity and mechanism of potassium cinnamate intended as a natural preservative. *LWT*. 2025, *215*, 117237. https://doi.org/10.1016/j.lwt.2024.117237

7. Zeleňák V., Císařová I., Llewellyn P. Diversity of carboxylate coordination in two novel zinc(II) cinnamate complexes. *Inorg. Chem. Comm*. 2007, *10*(1), 27–32. https://doi.org/10.1016/j.inoche.2006.08.021
8. Drew M. G. B., Mullins A. P., Rice D. A. Synthesis, characterization and structural properties of some copper(II) trans-cinnamates and related compounds. *Polyhedron*. 2007, *13*(10), 1631–1637. https://doi.org/10.1016/s0277-5387(00)83459-2
9. Kalinowska M., Świsłocka R., Lewandowski W. The spectroscopic (FT-IR, FT-Raman and 1H, 13C NMR) and theoretical studies of cinnamic acid and alkali metal cinnamates. *J. Mol. Struct*. 2007, *834–836*, 572–580. https://doi.org/10.1016/j.molstruc.2006.11.043
10. Crowther D., Chowdhury M., Kariuki B. M. Layering in cinnamate structures: The role of cations and anion substituents. *J. Mol. Struct*. 2008, *872*(1), 64–71. https://doi.org/10.1016/j.molstruc.2007.02.022
11. Mohsin S. M. N., Hussein M. Z., Sarijo S. H., Fakurazi S., Arulselvan P., Hin T.-Y.Y. Synthesis of (cinnamate-zinc layered hydroxide) intercalation compound for sunscreen application. *Chem. Central J*. 2013, *7*(26), 26. https://doi.org/10.1186/1752-153X-7-26
12. Kondratenko Y., Zolotarev A. A., Ignatyev I., Ugolkov V., Kochina T. Synthesis, crystal structure and properties of copper(II) complexes with triethanolamine and carboxylic acids (succinic, salicylic, cinnamic). *Transit. Metal Chem*. 2020, *45*(1), 71–81. https://doi.org/10.1007/s11243-019-00359-7
13. Batoola S. S., Gilani S. R., Zainab S. S., Tahir M. N., Harrison W. T. A., Haider M. S., Syed Q., Mazhar S., Shoai M. Synthesis, crystal structure, thermal studies and antimicrobial activity of a mononuclear Cu(II)-cinnamate complex with N,N,N′,N′ tetramethylethylenediamine as co-ligand. *Polyhedron*. 2020, *178*, 114346. https://doi.org/10.1016/j.poly.2020.114346
14. Sharma R. P., Saini A., Venugopalan P., Jezierska J., Ferretti V. Rare monomeric-dimeric copper(II) cinnamate complexes in one single crystal: Syntheses, characterization, structure determination and DFT studies of two copper(II) complexes. *Inorg. Chem. Comm*. 2012, *20*, 209–213. https://doi.org/10.1016/j.inoche.2012.03.010
15. Singh B., Singh R., Chaudhary R. V., Thakur K. P. Thioamide bands and nature of bonding in transition metal complexes of ligands having a thioamide group. *Indian J. Chem*. 1973, *11*(2), 174–177.
16. Neese F., Wennmohs F., Becker U., Riplinger C. The ORCA quantum chemistry program package. *J. Chem. Phys.* 2020, *152*(22), 224108. https://doi.org/10.1063/5.0004608
17. Becke A. D. Density-functional thermochemistry. III. The role of exact exchange. *J. Chem. Phys.* 1993, *98*(7), 5648–5652. https://doi.org/10.1063/1.464913
18. Lee C., Yang W., Parr R. G. *Development of the Colle-Salvetti correlation-energy formula into a functional of the electron density. Phys. Rev. B*. 1988, *37***(**2), 785–789. https://doi.org/10.1103/PhysRevB.37.785
19. Weigend F., Ahlrichs R. *Balanced basis sets of split valence, triple zeta valence and quadruple zeta valence quality for H to Rn: design and assessment of accuracy. Phys. Chem. Chem. Phys***.** 2005, *7***(18),** 3297–3305. https://doi.org/10.1039/B508541A
20. Barone V., Cossi M. *Quantum calculation of molecular energies and energy gradients in solution by a conductor solvent model. J. Phys. Chem. A***.** 1998, *102***(**11), 1995–2001. https://doi.org/10.1021/jp9716997
21. Lichtenecker K. *Die Dielektrizitätskonstante natürlicher und künstlicher Mischkörper. Physikalische Zeitschrift*. 1926, *27***,** 115–158.
22. Chemcraft — graphical software for visualization of quantum chemistry computations. Version 1.8, build 682. https://www.chemcraftprog.com
23. Hanwell M. D., Curtis D. E., Lonie D. C., Vandermeersch T., Zurek E., Hutchison G. R. "Avogadro: An advanced semantic chemical editor, visualization, and analysis platform". *J. Cheminformatics*. 2012, *4*(1), 17. https://doi.org/10.1186/1758-2946-4-17
24. Domingo L., Ríos-Gutiérrez M., Pérez P. Applications of the conceptual density functional theory indices to organic chemistry reactivity. *Molecules*. 2016, *21*(6), 748–770. https://doi.org/10.3390/molecules21060748

ORCID iDs
T. V. Koksharova: https://orcid.org/0000-0003-4295-2352
A. Yu. Kovalov: https://orcid.org/0009-0009-3278-5897